Journal of Controlled Release 309 (2019) 72–81

Contents lists available at ScienceDirect

Journal of Controlled Release

journal homepage: www.elsevier.com/locate/jconrel

Codelivery of paclitaxel and temozolomide through a photopolymerizable hydrogel prevents glioblastoma recurrence after surgical resection

Mengnan Zhao[a], Elia Bozzato[a], Nicolas Joudiou[b], Sina Ghiassinejad[c], Fabienne Danhier[a], Bernard Gallez[d], Véronique Préat[a,*]

[a] Université catholique de Louvain, Louvain Drug Research Institute, Advanced Drug Delivery and Biomaterials, Avenue Mounier, 73, B1.73.12, 1200 Brussels, Belgium
[b] Université catholique de Louvain, Louvain Drug Research Institute, Nuclear and Electron Spin Technologies Platform (NEST), Avenue Mounier, 73, B1.73.08, 1200 Brussels, Belgium
[c] Université catholique de Louvain, Institute of Condensed Matter and Nanoscience (IMCN), Bio and Soft Matter, Croix du Sud 1, B-1348 Louvain-la-Neuve, Belgium
[d] Université catholique de Louvain, Louvain Drug Research Institute, Biomedical Magnetic Resonance Research Group, Avenue Mounier, 73, B1.73.08, 1200 Brussels, Belgium

ARTICLE INFO

Keywords:
Glioblastoma
Nanomedicine
Nanoparticles
Local delivery
Hydrogel
Combination therapy

ABSTRACT

A photopolymerizable hydrogel-based local drug delivery system was developed for the postsurgical treatment of glioblastoma (GBM). We aimed for a local drug combination therapy with paclitaxel (PTX) and temozolomide (TMZ) within a hydrogel to synergistically inhibit tumor growth. The *in vitro* cytotoxicity of TMZ was assessed in U87MG cells. We demonstrated the synergistic effect of PTX and TMZ on U87MG cells by clonogenic assay. Treatment with TMZ did not induce O6-methylguanine-DNA methyltransferase related drug resistance in tumor-bearing mice. PTX had sustained release for at least 1 month *in vivo* in healthy mice brains. The drug combination was tolerable and suppressed tumor growth more efficiently than the single drugs in the U87MG orthotopic tumor model. The PTX and TMZ codelivery hydrogel showed superior antitumor effects and can be considered a promising approach for the postsurgical treatment of GBM.

1. Introduction

Glioblastoma (GBM) is the most malignant and frequently occurring tumor in the central nervous system, accounting for 16% of all central nervous system neoplasms [1]. GBM is an uncurable disease; 70% of GBM patients will experience disease progression within 1 year of diagnosis [2], with a median overall survival of 14 to 20 months in recent clinical trials [3,4]. Current gold standard treatments include massive safe surgical resection and subsequent radiotherapy with concurrent oral temozolomide (Temodar®, TMZ) followed by adjuvant chemotherapy with TMZ [5]. However, higher doses of TMZ were related to dose-limiting myelosuppression [6]. Due to the cellular and molecular heterogeneity of GBM, we were motivated to identify and characterize a combination agent inducing a synergistic effect with TMZ. Paclitaxel (PTX) is an efficient anticancer drug and has different mechanisms of action, non-overlapping toxicities and distinct mechanisms of resistance compared to TMZ [7]. We hypothesized that PTX could be a promising combination agent with TMZ.

Extensive and complete surgical resection of GBM is difficult, because GBM is often highly infiltrative. Additionally, the existence of the blood-brain barrier (BBB) prevents most oral and intravenous chemotherapeutic agents from reaching the tumor site [8]. GBM most commonly recurs within 2 cm of the resection border in the form of local continuous growth. Therefore, local brain treatment with antitumor chemotherapeutic agents can be administered after surgery to ensure the delivery of cytotoxic drugs to the remaining infiltrating tumor cells [9]. The only local delivery implant currently approved by the FDA is the Gliadel®, a carmustine-loaded polyanhydride copolymer wafer that has been shown to prolong the overall survival of patients to 16.4 months compared to 13.1 months for patients without wafers [10]. However, the cylinder-like structure of the wafer limits the close contact with the brain parenchyma and induces side effects, *e.g.*, infection and inflammation [10–12]. Among all local delivery systems, hydrogels are highly desirable. Cytotoxic drugs loaded in a hydrogel can be administered into the tumor resection cavity and adhere to the brain parenchyma [13]. The hydrogel matrix would ensure the sustained release of the loaded drugs. The ideal hydrogel delivery system for GBM has to meet the following requirements: sterile, injectable, adhesive to the resection cavity and biocompatible [13]. Recently, we reported a novel photopolymerizable hydrogel extraordinarily formed of

* Corresponding author.
E-mail address: veronique.preat@uclouvain.be (V. Préat).

https://doi.org/10.1016/j.jconrel.2019.07.015
Received 3 April 2019; Received in revised form 2 July 2019; Accepted 11 July 2019
Available online 12 July 2019

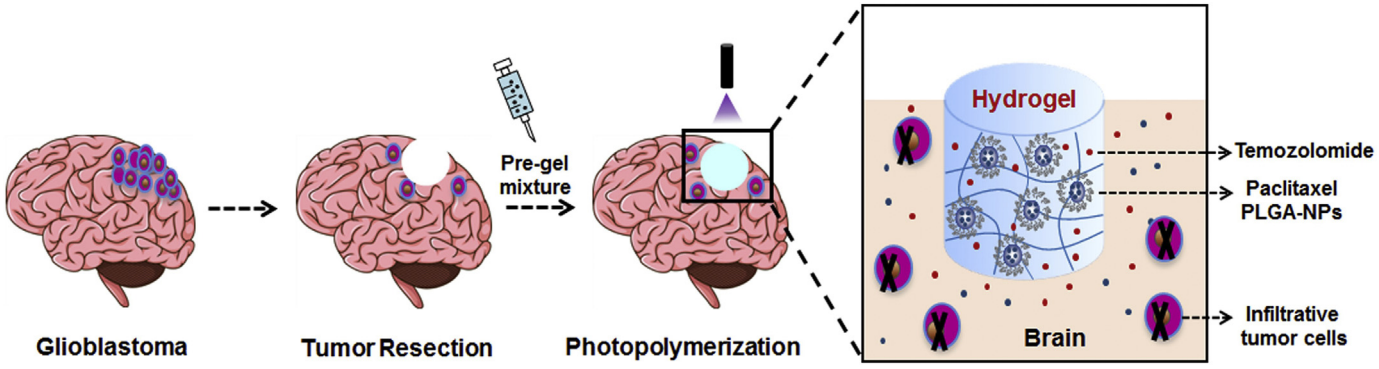

Fig. 1. Codelivery of PTX and TMZ through a photopolymerizable hydrogel for the postresection treatment of glioblastoma.

polyethylene glycol dimethacrylate (PEG-DMA) delivering PTX encapsulated in poly (lactic-co-glycolic acid) (PLGA) nanoparticles for the local administration of GBM treatment [14,15]. This injectable hydrogel system was suitable for brain tumor postresection implantation and allowed sustained drug release. This system was well tolerated in the mouse brain, inhibited tumor recurrence and led to long-term survival in the aggressive U87MG mouse model. This system can also be loaded with TMZ [14].

To further improve GBM treatment, the aim of the present study was to investigate the antitumor efficacy of this photopolymerizable hydrogel system loaded with the combination of TMZ and PTX (Fig. 1). The cytotoxicity, combination effect, drug resistance (O6-methylguanine-DNA methyltransferase, MGMT) after TMZ treatment, *in vivo* PTX diffusion, drug combination safety and antitumor efficacy in an orthotopic U87MG tumor resection model were investigated.

2. Materials and methods

2.1. Hydrogel preparation and characterization

2.1.1. Preparation of PTX PLGA-NPs and TMZ coloaded hydrogels (PTX PLGA-NPs/TMZ/PEG-DMA)

TMZ and L-histidine were purchased from Sigma-aldrich (USA). The same amounts of TMZ and L-histidine (w:w) were solubilized together in water to obtain a clear solution [16]. PTX PLGA-NPs were formulated using an emulsion-evaporation method as previously described [15]. The TMZ/L-histidine solution and the PTX PLGA-NPs were mixed together with a drug ratio of 2:1 (as illustrated in Section 3.3). Then, 75% (v:v) drug mixture was added to 25% PEG-DMA (average Mn = 550 g/mol) (Sigma-Aldrich) with Lucirin TPO® (BASF, USA) as a photoinitiator [15]. Then, the injectable pregel mixture was photopolymerized under 400 nm light. Single drug-loaded PEG-DMA hydrogels were also prepared by adding single drug formulations to the pregel mixture. For *in vivo* PTX diffusion assays, 15 μg/mL Oregon Green™ 488-PTX (Thermo Fisher, USA) -loaded PLGA-NPs were prepared by the same emulsion-evaporation method.

2.1.2. Mechanical properties of the PEG-DMA hydrogel

Rheological measurements were carried out with a Kinexus Pro rheometer (Malvern Instruments, UK). A parallel plate geometry of 8 mm in diameter was selected, and a constant 1 mm gap was maintained between the two plates. Ninety microliters of pregel mixture was introduced between the two plates. The light source was placed under the lower plate made of transparent glass. Immediately after placement of the pregel mixture, the plate cartridge was closed and a small amplitude oscillatory strain was applied to the sample, at a frequency of 10 rad/s and the strain amplitude of 1%, which was chosen in order to stay in the linear regime of deformation. The evolution of the storage modulus G′ and loss modulus G″ were investigated through time for a total time of 120 s, following a specific protocol: The first 10 s were used to determine the initial modulus. Then, lamp was turned on for 15 s, before turning it off for the remaining time of the experiment. Measurements were performed at 25 °C. The total crosslinking time of the hydrogel was defined as the time required to reach 95% of the maximum storage modulus following radical initiation. For swelling analysis, hydrogels after polymerization were incubated at 37 °C in phosphate-buffered solution (PBS, pH = 7.4). A line was drawn to show the initial volume of the pregel mixture. Gels were weighed before and after the 24 h immersion (n = 3).

2.2. In vitro cytotoxicity studies

2.2.1. Cell cultures

U87MG cell lines (ATTC, USA) were cultivated in Eagle's Minimum Essential Medium (EMEM) with 10% Fetal Bovine Serum (FBS) (Gibco, USA) and a 1% penicillin/streptomycin mixture (Gibco) (EMEM complete medium). Cells were cultured in 75 cm^2 culture flasks (Corning® T-75, Sigma-Aldrich) and incubated at 37 °C and 5% CO_2.

2.2.2. Clonogenic assay

The clonogenic assay for TMZ and combinations of TMZ and PTX on U87MG cells was adapted from Franken et al. [17]. Briefly, 1×10^5 U87MG cells were seeded per well in a 12-well plate and incubated at 37 °C with 5% CO_2 for 24 h. Cells were then incubated with different treatments for 48 h. Next, the cells were detached from the plate, and 300 cells were seeded in a 6-well plate with EMEM complete medium. At day 12, the medium was discarded, and the clones were fixed and stained by adding 50% ethanol, 5% acetic acid and 0.5% crystal violet for 30 min at room temperature. Then, the clones were washed twice with water and air dried. The numbers of colonies were counted by an automatic colony counter pen and compared with the untreated cells (n = 3).

2.2.3. Evaluation of the combination effect by the coefficient of drug interaction (CDI)

The combination effect was evaluated by the CDI, which was calculated as follows: CDI = AB/(A × B). AB is the numbers of colonies formed (% of control) of the combined effects of both drugs. A or B is the numbers of colonies formed (% of control) of each drug alone. [18]. The synergistic cytotoxicity was also confirmed by the CompuSyn software [19].

2.3. In vivo MGMT expression after TMZ treatment

In this experiment, U-251 and T98G cell lines were used as negative and positive controls, respectively. Mice bearing recurrent U87MG tumors after resection or TMZ treatment were sacrificed, and the brains were harvested. Total RNA was extracted from U87MG cells and tumor tissues using Trizol (Invitrogen, USA) plus an RNA purification system (Thermo fisher). Reverse transcription PCR was performed with

isolated and purified total RNA and synthesized to cDNA in a 20 μL reaction system using reverse transcriptase (Promega, USA) with oligo-dT primers according to the manufacturer's instructions. cDNA was obtained to determine MGMT expression after amplification with the following primers: Fw 5′- GGA GGC ACC GCT GTA TTA AA -3′ and Rv 5′- GCA GGT AGG AAA CAA AGC TAG A -3′ [20]. Human-derived β-actin was the endogenous control. PCR was performed under classical conditions with the initial denaturation for 3 min at 94 °C; 30 total cycles of 1 min denaturation at 94 °C and annealing for 1 min at 55 °C, followed by extension for 1 min at 72 °C; and a final extension step of 7 min at 72 °C. Amplified products were separated by electrophoresis on a 1% agarose gel and visualized under UV illumination ($n = 3$). MGMT levels against actin were determined by image J software.

2.4. In vivo studies

All the experiments were performed following the Belgian national regulation guidelines in accordance with EU Directive 2010/63/EU and were approved by the ethical committee for animal care of the Université catholique de Louvain medicine faculty (2014/UCL/MD/004). Animals had free access to water and food, and the body weights were monitored daily throughout the experiments.

2.4.1. Orthotopic U87MG human GBM tumor resection model

Six-week-old NMRI female nude mice (Janvier, France) were anesthetized by intraperitoneal injection of ketamine/xylazine (100 and 13 mg/kg, respectively) and positioned on a stereotactic frame as previously described [21]. A five-microliter Hamilton syringe with a 26 G needle was used to inject up to 3 μL of complete culture medium containing 3×10^4 U87MG glioma cells into the right frontal lobe. The injection site was 0.5 mm anterior, 2.1 mm lateral from the bregma and 2.5 mm deep from the cranium. After 13 days, the cranium was opened again, and a 2 mm diameter biopsy punch (Kai Medical, Germany) was inserted 3 mm deep and twisted for 15 s to cut the tumor tissues. Then, the tumor tissues were aspirated using a diaphragm vacuum pump. Five microliters of hydrogel was photopolymerized into the resection cavity before closing the cranial window with a 4 mm × 4 mm Neuro-Patch® (Aesculap, Germany) saturated with a reconstituted fibrin glue (Baxter Innovations, Austria).

2.4.2. In vivo local PTX diffusion

Six-week-old healthy female Swiss mice (Janvier) were anesthetized and positioned in a stereotactic frame. Five microliters of hydrogel loaded with 15 μg/mL Oregon Green™ 488-PTX (Thermo Fisher) within PLGA-NPs was photopolymerized into the resection cavity before sealing the cranial window with a 4 mm × 4 mm square piece of Neuro-Patch® impregnated with a reconstituted fibrin glue (Baxter Innovations). Animals were then sacrificed at 0 h, 24 h, 96 h, 10 days or 1 month after hydrogel injection. The brain was rapidly harvested and embedded in OCT on dry ice. Brains were cryosectioned using a Leica 1950 cryostat (Leica, Germany) into 40 μm thick slices and stained with DAPI (2 μg/mL, nuclear stain) (Thermo Fisher). Images were acquired on Zeiss LSM 710 and Zeiss BF/LF Axio Imager microscopes, and the analyses were processed in a ZEN 2.5 (Zeiss, Germany) system ($n = 3$–6).

2.4.3. In vivo safety study of the drug combination

Six-week-old healthy female NMRI nude mice (Janvier) were anesthetized intraperitoneally. Normal brain resections were performed using the biopsy punch resection model as described in Section 2.4.1. The *in vivo* safety evaluation of the drug combination was conducted by injecting the treatment in the brain resection cavity as follows: resection group ($n = 5$); resection and unloaded PEG-DMA hydrogel implanted group ($n = 5$); resection, PTX PLGA-NPs and TMZ coloaded PEG-DMA hydrogel implanted group ($n = 5$). The doses of PTX and TMZ administered were 0.3 mg/kg and 0.6 mg/kg, respectively. After 1 month, brains were cryosectioned using a Leica 1950 cryostat into 15 μm thick slices. Hematoxylin and eosin (H&E) and Iba-1 immunohistochemistry were performed as previously described [9,15]. Slides were scanned using an SCN400 Leica slide scanner, and image analysis was performed on a selected zone with Digital Image Hub (Leica).

2.4.4. Immunostaining of tumor-bearing and tumor-resected brains

All the treatments were tested on the U87MG orthotopic model described in Section 2.4.1. After tumor injection, the tumor-bearing brains (days 13 and 36) and the tumor-resected brains (day 13) were sectioned with a Leica CM 1950 cryostat into 15 μm thick slices and stored at −20 °C until use. The positive controls were the sections of brain with tumors on day 36. As described previously [14,21], the day 13 tumor-bearing brains were evaluated by immunostaining with anti-human mitochondria antibody and anti-glial fibrillary acidic protein (GFAP) antibody (Thermo Fisher). After tumor resection, proliferative tumor cells were detected using an anti-Ki67 monoclonal antibody (Thermo Fisher). The nucleus was counterstained with hematoxylin. The brain digital images were acquired using an EVOS fluorescence microscope (Evos, USA) and Digital Image Hub ($n = 3$).

2.4.5. In vivo antitumor efficacy of PTX PLGA-NPs/TMZ coloaded PEG-DMA hydrogels on the orthotopic U87MG tumor resection model

Tumor resection was performed using the biopsy punch resection model described in Section 2.4.1. The *in vivo* antitumor efficacy of the drug combination was determined on day 13 post tumor injection by administration of the following treatments in the tumor resection cavity: untreated group ($n = 7$); resection and untreated group ($n = 8$); resection and PTX PLGA-NP-loaded PEG-DMA hydrogel treated group ($n = 6$); resection and TMZ-loaded PEG-DMA hydrogel treated group ($n = 6$); resection and PTX PLGA-NPs and TMZ coloaded PEG-DMA hydrogel treated group ($n = 9$). The doses of PTX and TMZ were 0.3 mg/kg and 0.6 mg/kg, respectively. Mice were sacrificed when they presented a 20% body weight loss or 10% body weight loss associated with clinical signs of distress (paralysis, arched back, or apathy). The rest of the mice were sacrificed 110 days after tumor implantation. The size and location of the tumors were determined by T2-weighed magnetic resonance imaging (MRI) using an 11.7 T Bruker BioSpec MRI system (Bruker, Germany) for all mice 12 days post tumor cell implantation and before being sacrificed as previously described [15].

2.5. Statistical analysis

All the *in vitro* experiments were performed at least three times with three replicates each time ($N = 3$, $n = 3$). The results are expressed as the mean ± standard deviation (SD) or the mean ± standard error (SEM). Statistical analysis was performed using GraphPad Prism for paired *t*-test and ANOVA. *In vivo* Kaplan–Meier survival analysis was performed using log-rank test. The significance was set to probabilities of $*p < .05$, $**p < .01$, and $***p < .001$ when compared with controls.

3. Results and discussions

3.1. In vitro characterization of the PEG-DMA hydrogel

The resulting PTX PLGA-NPs were 190 ± 4 nm in size. Twenty-five percent PEG-DMA (v:v) was chosen to ensure hydrogel formation with a higher drug amount (Fig. S1). To investigate the crosslinking kinetics and rheological properties of the hydrogels, rheological time-sweep tests were performed. Fig. 2 shows the evolution of the storage modulus (G') over the time course of gel formation when irradiated with 400 nm light. It was observed that only 15 s of light exposure can initiate the fast curing process. The total crosslinking time of the hydrogel is 66 s for the gel with or without nanoparticles. The final storage modulus G′

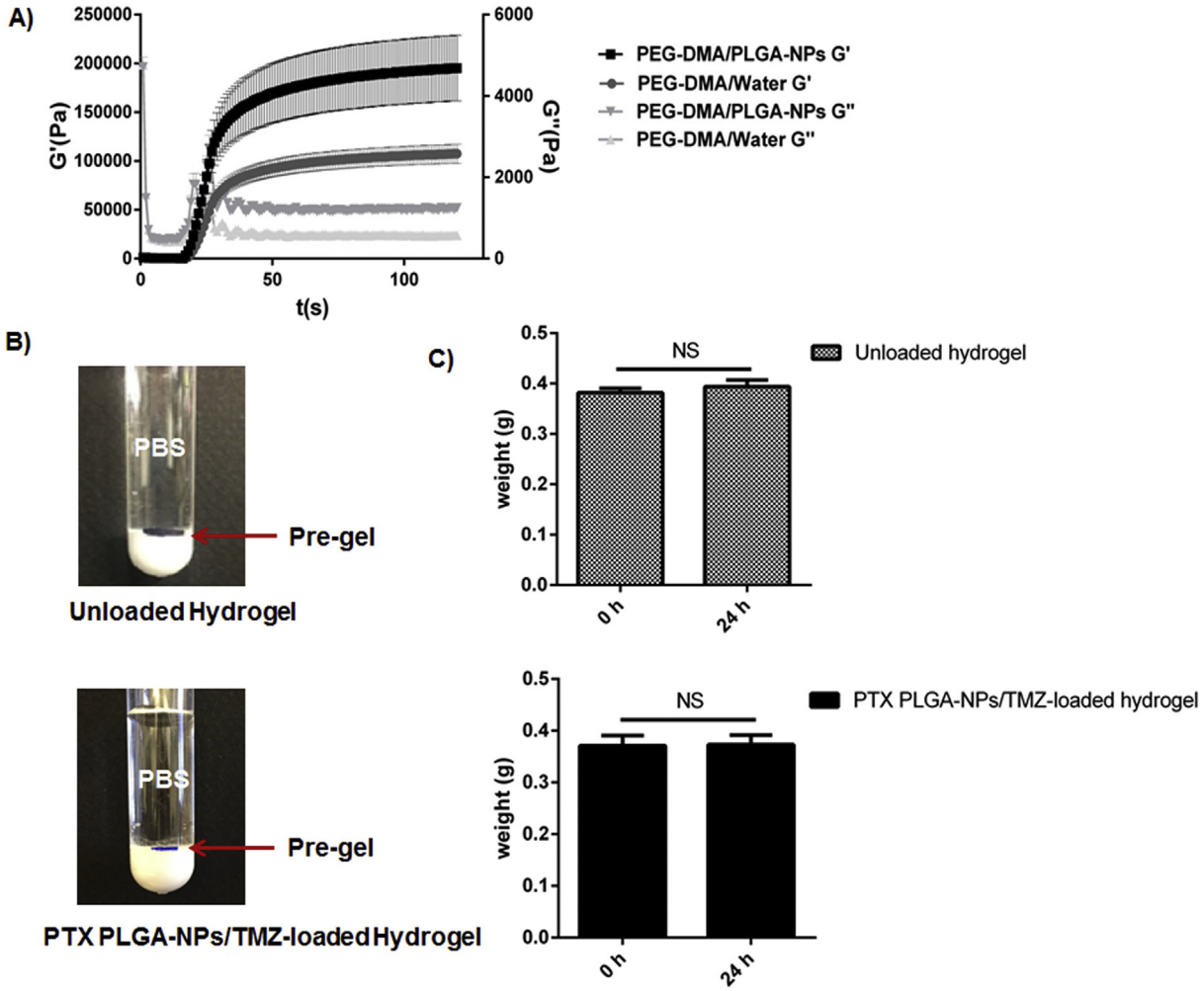

Fig. 2. *In vitro* hydrogel characterizations. (A) Storage (G′) and loss modulus (G″) during photopolymerization were measured. Mean ± SEM, $n = 3$. (B) After immersing in PBS for 24 h, the volume of unloaded or drug coloaded hydrogels remained same as compared with the pregel mixture. (C) The weights of hydrogel before and after immersing in PBS for 24 h were also measured. Mean ± SD, $n = 3$.

(elastic behavior) of PEG-DMA/PLGA-NPs and PEG-DMA/water (195.3 ± 58.2 kPa and 107.3 ± 16.9 kPa, respectively) was significantly higher than that of the loss modulus G″ (viscous behavior) (1.25 ± 0.14 kPa and 0.58 ± 0.03 kPa, respectively) ($p < .05$). This result indicates that elasticity dominates in all samples, which is a typical behavior of solid-like materials. The storage modulus is directly related to the extent of crosslinking; the higher the degree of crosslinking, the greater the storage modulus. Although the storage modulus of hydrogel is higher than the brain storage modulus (0.6 to 22.1 kPa) [22], the tolerability studies conducted at 1 week, 2 months and 4 months indicated that the gel did not increase microglia activation and apoptosis compared to the lesion after resection [14,15], suggesting that the mechanical properties are acceptable. To avoid an increase in intracranial pressure, gel swelling must be avoided. No significant change was observed in hydrogel mass ($p > .05$) or gel volume after 24 h, indicating that the unloaded or drug coloaded PEG-DMA hydrogels had a low swelling capacity and that the volume of the pregel mixture remained the same as the final solid hydrogel.

3.2. In vitro cytotoxicity of TMZ on U87MG cells

As the *in vitro* cytotoxicity effects of PTX were already performed in previous work [15], we focused only on the cytotoxicity of TMZ. The preliminary study was conducted with the MTT assay (Fig. S2). An IC_{50} of TMZ (841 μg/mL) was obtained (Fig. S2A). However, we found a dose-dependent interaction between TMZ and MTT (Fig. S2B). Next, crystal violet was chosen because it is enzyme-independent and directly measures the DNA mass of adherent cells [23]. Crystal violet staining was performed after 48 h of incubation with TMZ. As shown in Fig. S2C, the IC_{50} value of TMZ was 397 μg/mL. Some authors have previously evaluated the cytotoxic effects of TMZ on GBM cells, and the IC_{50} values varied between 1.4 μg/mL and 111 μg/mL [24–26]. However, the IC_{50} we obtained was higher than most of the reported values.

To find a better method to study TMZ cytotoxicity, a clonogenic assay was conducted. The resulting IC_{50} (2.4 μg/mL) dramatically decreased compared to that of crystal violet or MTT assays after incubation with lower TMZ concentrations (from 0.024 to 100 μg/mL in Fig. 3A). This indicates that the sensitivity of U87MG cells to TMZ was more pronounced in the clonogenic survival assay. For the following experiment, a clonogenic assay was chosen to investigate the combination effects of the two drugs.

3.3. In vitro combination effects of PTX and TMZ on U87MG cells

Combination therapy with anti-cancer drugs can act synergistically, additionally or antagonistically against tumor cell growth depending on the ratios of the drugs that composing the combination [27]. Thus, to investigate the combination effects of PTX and TMZ at different ratios, cells were treated with different drug concentrations selected based on the IC_{50} values. In Fig. 3B, the PTX and TMZ combination group showed

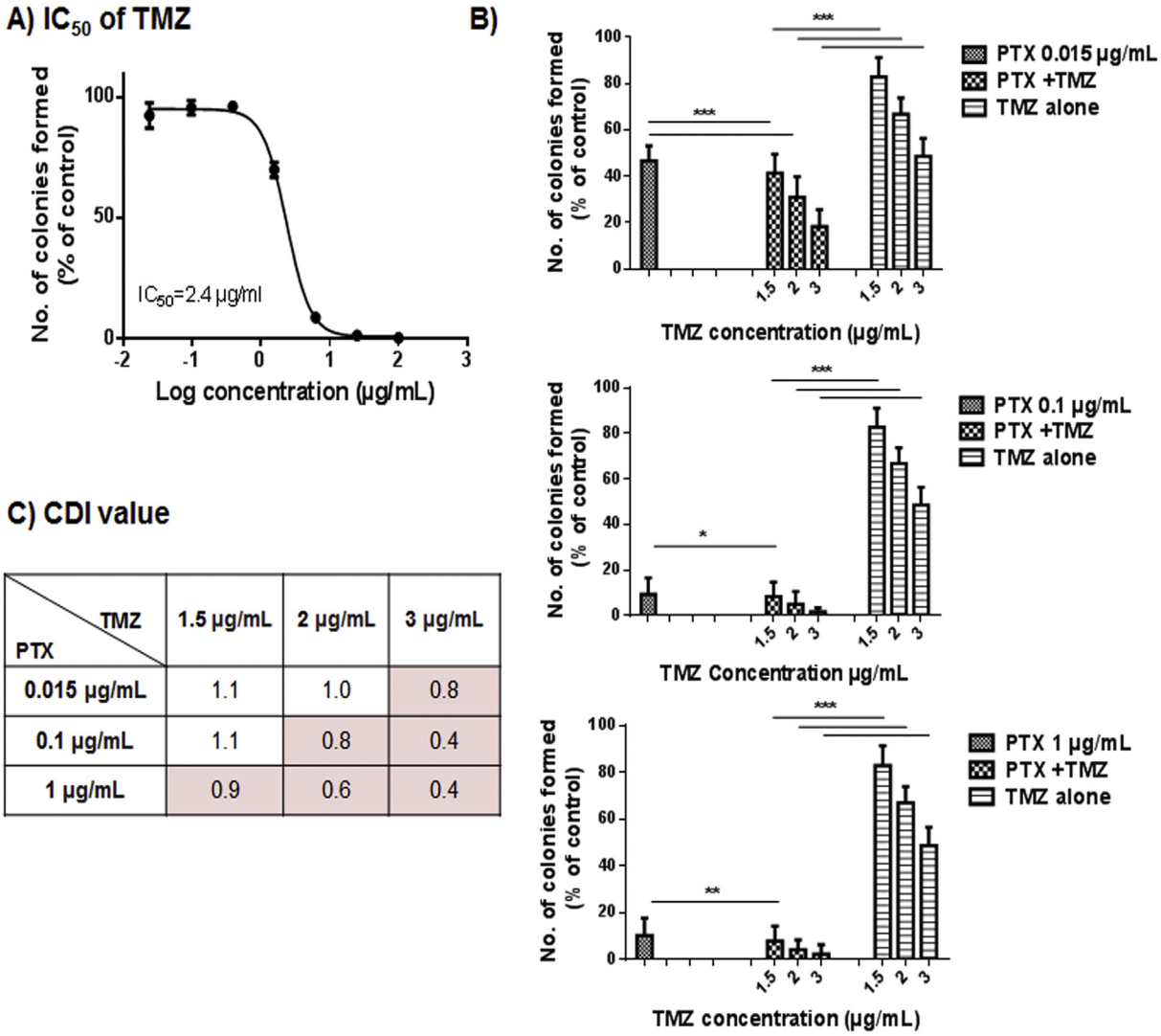

C) CDI value

PTX \ TMZ	1.5 μg/mL	2 μg/mL	3 μg/mL
0.015 μg/mL	1.1	1.0	0.8
0.1 μg/mL	1.1	0.8	0.4
1 μg/mL	0.9	0.6	0.4

Fig. 3. The cytotoxic effect of TMZ (A) and the combination effect of PTX in PLGA-NPs and TMZ (B) were assessed by clonogenic assay. U87MG glioma cells were treated for 48 h with TMZ at different concentrations. Mean ± SEM, $n = 3$, $^{*}p < .05$, $^{**}p < .01$, $^{***}p < .001$. Data are presented as the numbers of colony formation (untreated cells assumed as 100%). The CDI value was calculated to present the combination effect (C).

significantly higher cytotoxicity than TMZ alone. Although not all combinations showed significant differences compared with PTX alone, there were fewer colonies formed after the treatment by drug combination than by PTX alone. A CDI < 1, =1 or > 1 indicates that the drug combination has a synergistic, additive or antagonistic effect [18]. From Fig. 3C, the combination of PTX and TMZ at all concentrations tested showed that PTX and TMZ had additive or synergistic effects. To confirm these results, the combination effect was also evaluated with the software CompuSyn [19]. The CI value obtained was comparable with the CDI value calculated above (data not shown). Due to the limited solubility of TMZ, the highest TMZ concentration was 4 mg/mL. To load as much PTX as possible while maintaining a synergistic effect, we chose a concentration ratio of 1:2 (PTX to TMZ) for the *in vivo* study.

3.4. In vivo MGMT expression after TMZ treatment

The critical lethal lesion O6-alkylguanines induced by TMZ is neutralized in GBM by the DNA repair protein MGMT [28]. Thus, MGMT mRNA expression was investigated to determine whether TMZ resistance occurred after exposition of the tumors to TMZ. The expression of MGMT varies depending on different cell lines [29,30]. As shown in Fig. 4, U-251 and U87MG are TMZ-sensitive cell lines, as almost no MGMT expression were detected, while T98G is a TMZ-resistant cell line. The semi-quantitative analysis using Image J software demonstrated that the *in vivo* treatment with the TMZ-loaded hydrogel did not up-regulate the MGMT mRNA expression as compared with the untreated resected tumors. Some research has indicated that the promoter region for the MGMT gene in U87MG cells is methylated; thus, MGMT expression is silenced [31]. This finding could explain why treatment with TMZ did not increase MGMT expression. It has been reported that the establishment of the U87 TMZ-resistant glioma cell lines required exposure to gradually increasing concentrations of TMZ in culture media for 6 months [32]. However, under our experimental conditions, most of the TMZ was released within 1 week, and the drug release rate gradually decreased [14], suggesting that local treatment with the TMZ hydrogel would not induce drug resistance.

3.5. In vivo local PTX diffusion

To assess *in vivo* PTX diffusion from the hydrogel to the surrounding brain tissue, we administered an Oregon Green™ 488 conjugated PTX PLGA-NP-loaded PEG-DMA hydrogel into the mouse brain. As shown in Fig. 5A and B, no visible green fluorescence was found within the surrounding brain tissue at 0 h and 24 h, indicating that PTX did not

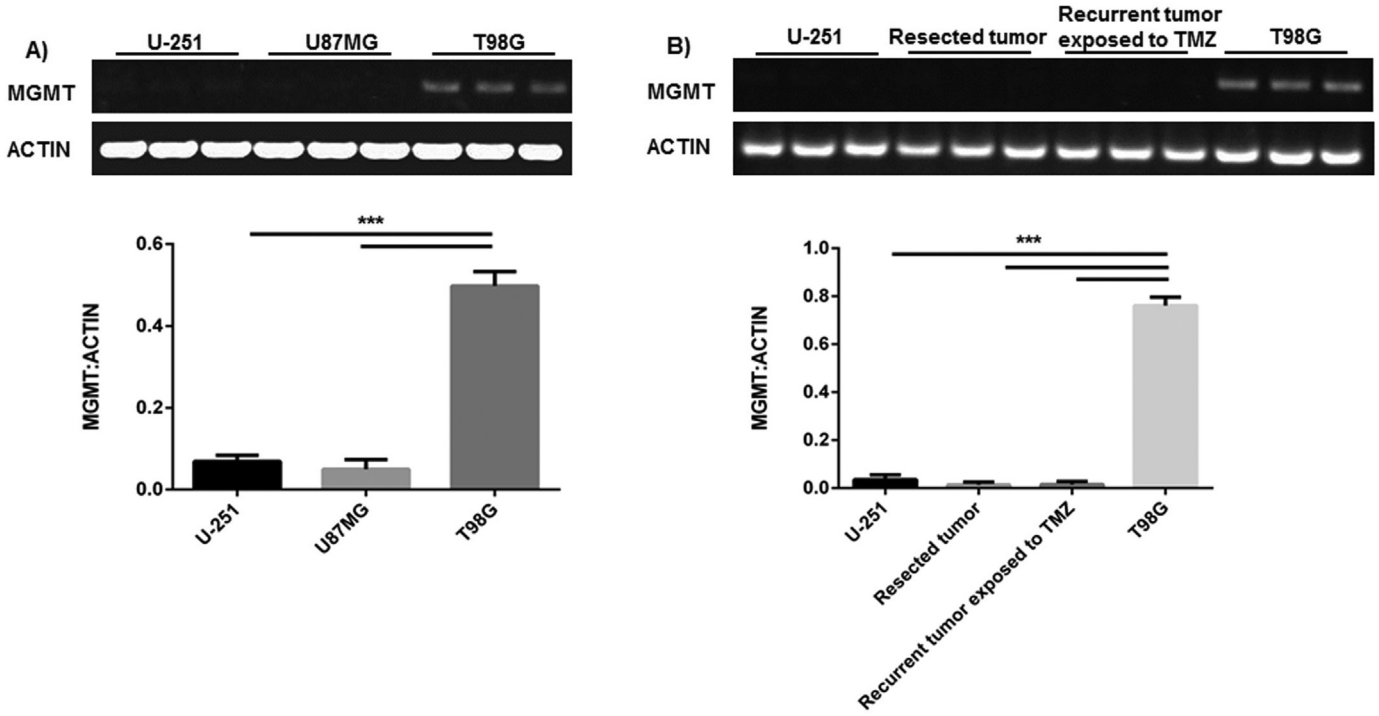

Fig. 4. MGMT expression in U87MG cells (A), resected tumor without treatments in 3 mice brains and recurrent tumor exposed to TMZ in 3 mice brains (B) were investigated by RT-PCR. U-251 and T98G cell lines were the negative and positive controls, respectively. Each MGMT levels against actin were determined by image J software. Mean ± SD, $n = 3$, ***$p < .001$.

diffuse through the resection border. Oregon Green™ 488 PTX was observed both within and outside the hydrogel at 96 h and 10 days post administration (Fig. 5C and D). In Fig. 5E, the Oregon Green™ 488-conjugated PTX signal remained outside the hydrogel after 1 month. The drug diffusion was not uniform at every gel-brain border. A strong burst release of PTX adsorbing to the surface of NPs must be avoided because it reduces the sustained release. In our case, PTX slowly diffused through the hydrogel; thus, in contrast to *in vitro* studies that showed that after an initial burst release, 30% of PTX was slowly released in a sustained manner over 1 week [15], almost no burst release was found 24 h post hydrogel injection. The sustained drug release lasts for at least 1 month, making this hydrogel a potential drug delivery system to fill in the 1 month wound-healing gap in the GBM standard treatment strategy [13].

The *in vivo* brain distribution of FITC-labeled PLGA-NPs within the hydrogel (Fig. S3) showed that the NPs were entrapped inside the hydrogel after 24 h and did not diffuse away. This result occurred because the NPs are noncovalently immobilized in the nondegradable hydrogel. To support this hypothesis, the mesh size (nm) was calculated from the molecular weight between two crosslinking points and the swelling experiment [33]. The mesh size in our hydrogel is approximately 10 nm. This could explain why the PLGA nanoparticles (190 nm size) were not able to diffuse out of the hydrogel. Thus the *in vitro* release profile of the NPs was not studied.

3.6. In vivo safety study of the drug combination

The potential toxicity of the PTX PLGA-NPs/TMZ/PEG-DMA hydrogel was evaluated after 1 month of exposure *via* local administration to the healthy mouse brain at doses of 0.3 mg/kg and 0.6 mg/kg for PTX and TMZ, respectively. As shown in Fig. S4, there was no significant difference in body weight and water and food consumption witnessed in the PTX PLGA-NPs/TMZ/PEG-DMA hydrogel group compared to the unloaded hydrogel or resection groups during this experiment. As shown in Fig. 6, microglial activation was observed in all groups and could generate reactive oxygen species and release signals to recruit peripheral immune cells. Biopsy punch resection can cause positive staining of the microglia activation marker Iba-1 [15]. The hydrogel alone and the drug coloaded hydrogel did not increase the extent of microglial activation compared to the resected group. No lethal brain damage was observed from the H&E staining of brain sections. In conclusion, hydrogels loaded with PTX and TMZ at doses of 0.3 mg/kg and 0.6 mg/kg, respectively, were tolerable for local administration in mouse brains.

3.7. In vivo antitumor efficacy of PTX PLGA-NPs/TMZ coloaded PEG-DMA hydrogels on an orthotopic U87MG tumor resection model

Immunostaining with an anti-human mitochondria antibody to detect human U87MG and an anti-GFAP antibody to detect brain tissue were performed on day 13 in tumor-bearing mouse brains. An anti-Ki67 antibody was employed to detect proliferating tumor cells just after tumor resection. A day 36 tumor was the positive control. As shown in Fig. 7A, the growth of human U87MG tumor cells could be identified by an anti-human mitochondria antibody (green). At the tumor-brain border, the tumor cells and brain tissues (red) were intertwined, and some tumor cells infiltrated into the brain parenchyma. Ki67-positive tumor cells (brown) were found in the main tumor mass of the day 36 tumor (Fig. 7B) and in the resection border of the day 13 tumor (Fig. 7C). Some infiltrative tumor cells were found far from the resection cavity after the removal of the tumor (Fig. 7D). These infiltrative tumor cells are likely to induce tumor recurrence after biopsy punch resection. After implantation of the hydrogel for > 3 months, some cells can be observed at the interface between the hydrogel and the cavity border but none inside the hydrogel (Fig. 7E).

To evaluate the antitumor efficacy of the PTX PLGA-NPs/TMZ coloaded hydrogel and its capacity to reduce tumor recurrence, treatments were intraoperatively injected into the resection cavity. As shown in Fig. 8A, we checked that all mice developed a tumor that was well-demarcated and visible by MRI imaging on day 12 post tumor cell

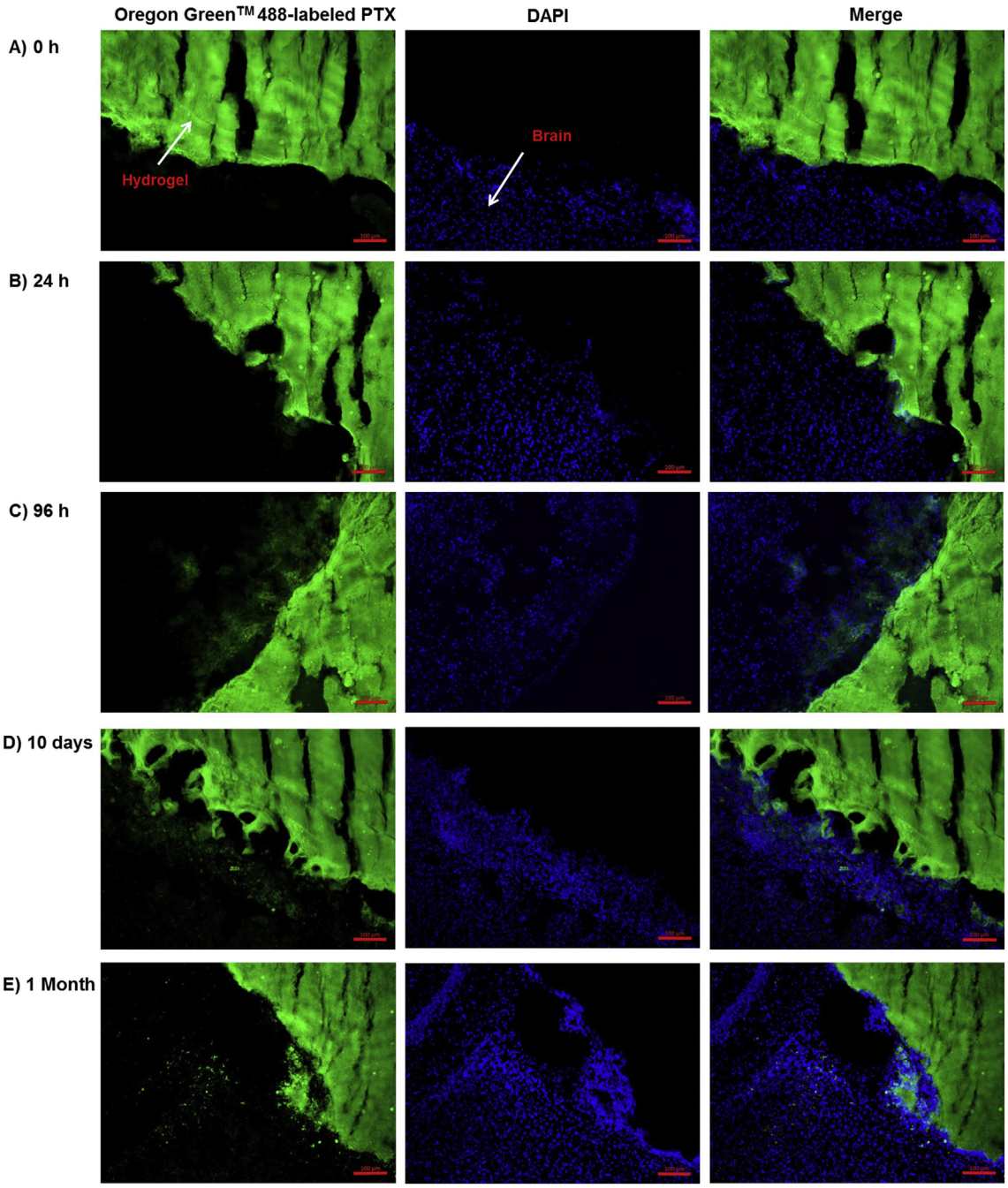

Fig. 5. *In vivo* local PTX diffusion was conducted with Oregon Green™ 488-labeled PTX (green) PEG-DMA hydrogels containing PLGA-NPs in healthy mouse brains. The nuclei were stained with DAPI (blue). Scale bar = 100 μm (n = 3–6). (For interpretation of the references to colour in this figure legend, the reader is referred to the web version of this article.)

injection. The hydrogel remained in place during the entire course of the experiment (Fig. 8B). The ester groups in PEG-DMA are susceptible to be degradable slowly *in vivo* [34,35]. The PLGA is also degradable *via* hydrolysis over months [36]. As no inflammation or cell death was observed (Fig. 7E and F), the remaining of the hydrogel in the cavity for > 3 months was not an issue.

As shown in Fig. 8C and D, injection of single drug treatment with PTX PLGA-NPs or TMZ-loaded hydrogels in the resection cavity significantly prolonged the median survival time of mice compared to that of the resected mice ($p < .05$ and $p < .01$, respectively). The combination treatment showed higher significance level compared to the other groups ($p < .001$), with an undefined median survival. Only 2 out of 9 mice had tumor recurrence within 110 days after injection of the tumor cells. The rest of the mice showed no sign of tumor recurrence by MRI imaging (Fig. S5) and H&E staining of the brain tissues (*e.g.* Fig. 7F). Among the 7 surviving mice, 2 brains showed edema around the resection cavity, which did not influence the behavior of the mice. These data suggest that the PTX and TMZ could diffuse from the hydrogel to avoid most of the recurrences.

It is well-known that the combination of chemotherapeutic drugs with different mechanisms of action may contribute to better antitumor effects. Here, PTX and TMZ have different mechanisms of action, resistance and established efficacy in glioma cells [37–39]; thus, the expected survival enhancement was observed in our results. In addition, clinical trials have demonstrated that the combination of PTX or docetaxel with TMZ has a synergistic effect in metastatic melanoma

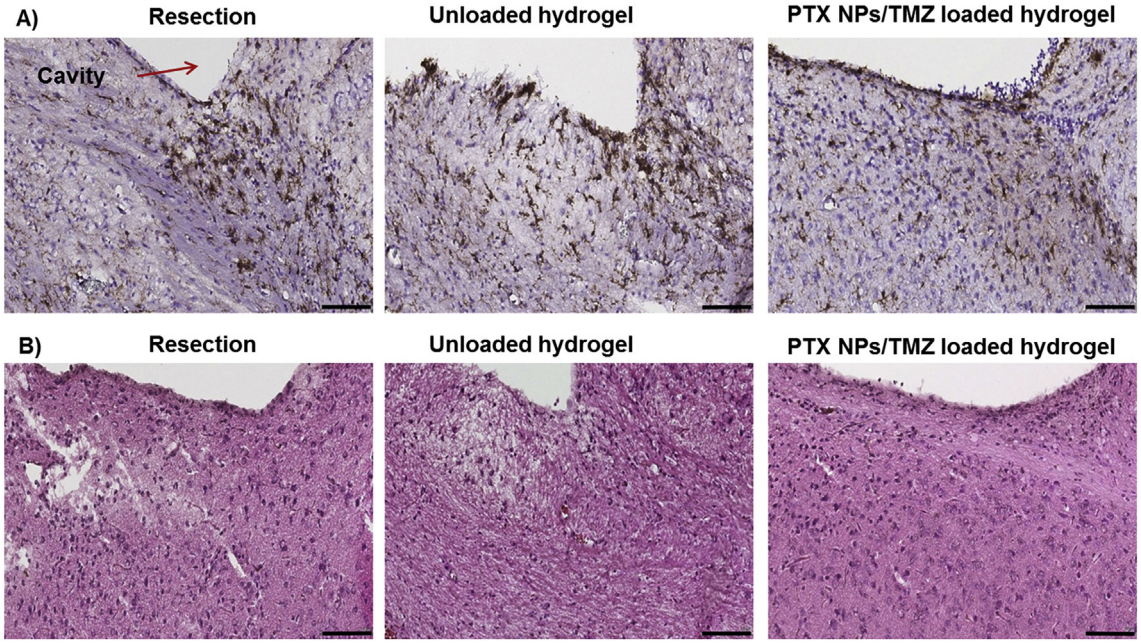

Fig. 6. *In vivo* safety study of drug combination: evaluation of microglia activation by Iba1 staining (brown) (A) and brain structure by H&E staining (B) in the brain tissue 1 month after treatment with different groups (resection, resection + unloaded hydrogel and resection + PTX NPs/TMZ coloaded hydrogel). The doses of PTX and TMZ were 0.3 mg/kg and 0.6 mg/kg, respectively. Scale bar = 100 μm (n = 3). (For interpretation of the references to colour in this figure legend, the reader is referred to the web version of this article.)

[40–42], making this combination a reasonable option for GBM treatments. The synergistic effect of PTX and TMZ on GBM cell lines has been investigated *in vitro* [38,39,43], but barely studied in the form of a local combination therapy in orthotopic models. Robert Clark equations is used to calculate the *in vivo* synergism based on the median survival [44]. However, as the median survival of combination treatment was undefined due to the long term survivors, we were not able to measure the *in vivo* synergism with our current data. In one study, the PEG-dipalmitoylphosphatidyle-thanoiamine calcium phosphate nanoparticles injectable thermo-responsive hydrogel was developed to sustain the local delivery of PTX and TMZ for only 3 days [45]. Although this thermo-responsive hydrogel induced significant therapeutic efficacy, all of the treatment groups had tumor recurrences and no animal survived for long-term. Our findings indicate that the combination group showed most significantly survival benefits in the U87MG tumor resection model and highlight the local combination option of PTX and TMZ as a promising strategy for GBM therapy.

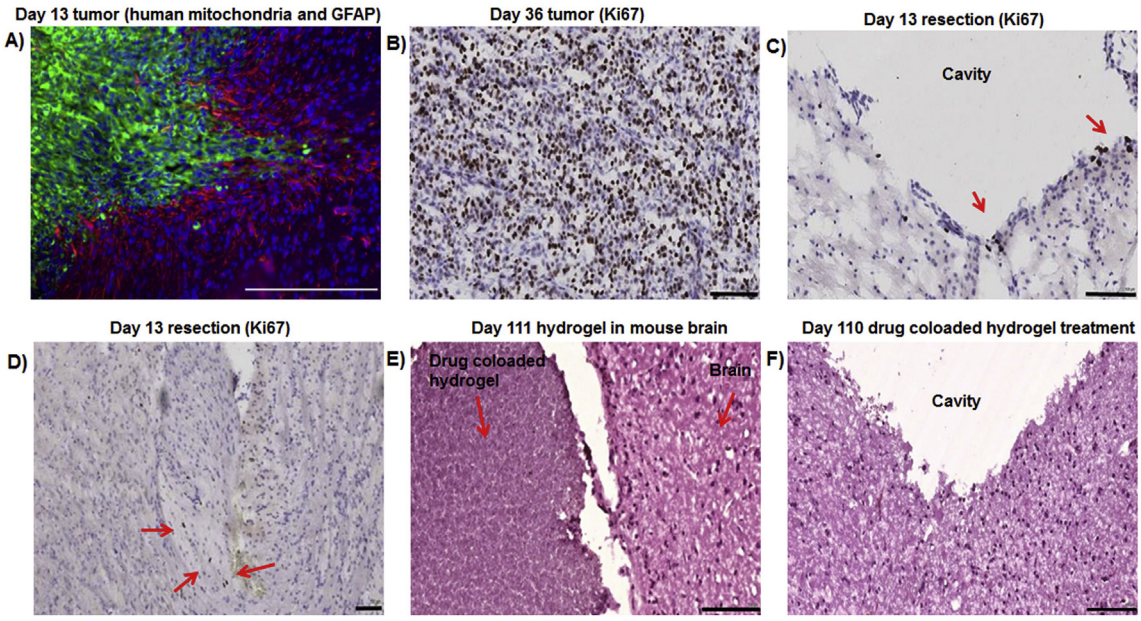

Fig. 7. (A) Anti-GFAP (red) with anti-human mitochondria staining (green) shows normal brain parenchyma and the day 13 tumor mass. Scale bar = 200 μm. (B-D) Anti-Ki67 staining (brown) with hematoxylin (blue) counterstaining shows the tumor cells in a day 36 recurrent tumor mass without resection (B) and day 13 tumor resection cavities in 2 different mice brains (C and D). n = 3. (*E*-F) H&E staining of 2 mice brains shows no infiltrative cells inside the drug coloaded hydrogel (E) and no tumor recurrence after treatment with drug coloaded hydrogel (F) on day 111 and 110 post tumor inoculation. Scale bar = 100 μm. (For interpretation of the references to colour in this figure legend, the reader is referred to the web version of this article.)

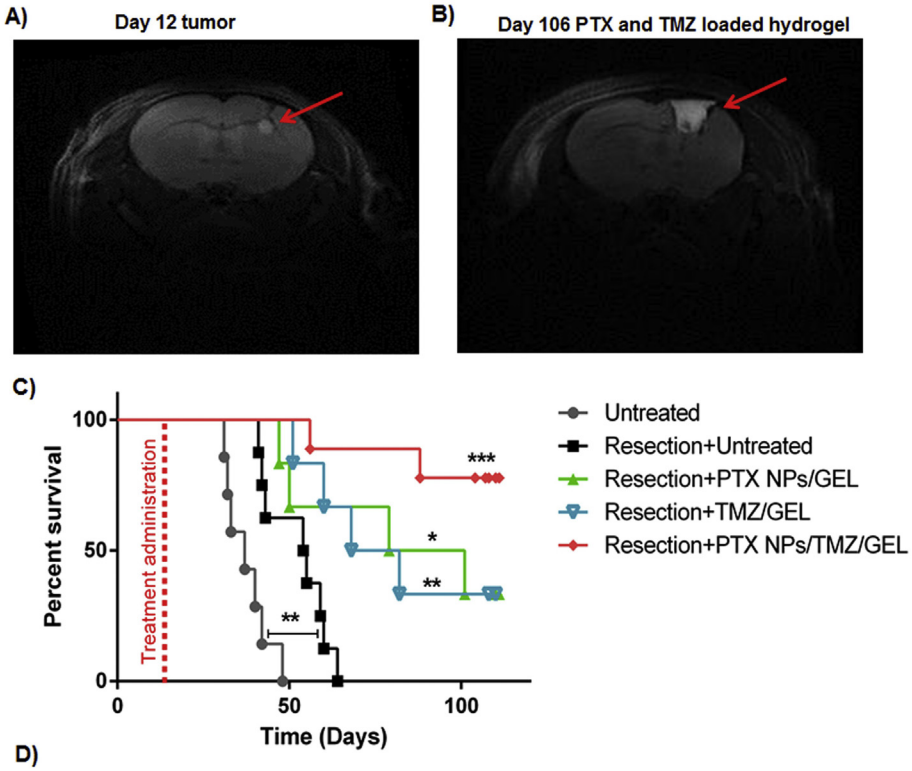

D)

Treatment	*n*	Median survival (days)	Log-rank test
Untreated	7	37	
Resection + untreated	8	54.5	** (*vs* untreated)
Resection + PTX NPs/Hydrogel	6	90	* (*vs* Resection + untreated)
Resection + TMZ/Hydrogel	6	75	** (*vs* Resection + untreated)
Resection + PTX NPs/TMZ/Hydrogel	9	Undefined	*** (*vs* Resection + untreated)

Fig. 8. Axial (T2-weighted) images of a mouse brain: tumor before resection (day 12 post tumor inoculation) (A) and the same brain treated with drug coloaded PEG-DMA hydrogel on day 106 post tumor inoculation (B). Kaplan-Meier survival curves (C) and median survival (D) for animals treated with different therapies in the resection cavity. $n = 6–9$, *p < .05, **p < .01, ***p < .001.

4. Conclusions

In conclusion, to address the unmet medical need for the treatment of recurrent GBM after surgery, we developed a local combination treatment strategy with PTX and TMZ based on the photopolymerizable PEG-DMA hydrogel. We demonstrated the synergistic effect of PTX and TMZ on U87MG cells by clonogenic assay. We also confirmed that TMZ treatment did not up-regulate MGMT expression in U87MG tumor-bearing mice. PTX release was sustained *in vivo* and diffused from the hydrogel to the surrounding brain tissue for at least 1 month. The local combination of PTX with TMZ was safe, effective and synergistic in the treatment of the U87MG orthotopic model. Although combination therapy protocols are becoming an integrated part of cancer treatment, rational and efficient combination therapy to improve the treatment of GBM remains limited. We showed that a rational combination of drugs and their rational, perisurgical delivery in the resection cavity of GBM led to long term survivors in mice. Future preclinical studies may take advantage of the potential benefits of this local combination treatment strategy. Clinical studies may also take PTX and TMZ into consideration as potential drug combination options.

Acknowledgments

This study was supported by the Université catholique de Louvain and the China Scholarship Council (CSC) (Mengnan Zhao). This work was also supported by a grant from the Fondation contre le Cancer (Belgium). The authors declare no conflict of interest.

Appendix A. Supplementary data

Supplementary data to this article can be found online at https://doi.org/10.1016/j.jconrel.2019.07.015.

References

[1] M.E. Davis, Glioblastoma: overview of disease and treatment, Clin. J. Oncol. Nurs. 20 (2016) S2.
[2] R. Stupp, W.P. Mason, M.J. van den Bent, M. Weller, B. Fisher, M.J.B. Taphoorn,

K. Belanger, A.A. Brandes, C. Marosi, U. Bogdahn, J. Curschmann, R.C. Janzer, S.K. Ludwin, T. Gorlia, A. Allgeier, D. Lacombe, J.G. Cairncross, E. Eisenhauer, R.O. Mirimanoff, Radiotherapy plus concomitant and adjuvant temozolomide for glioblastoma, N. Engl. J. Med. 352 (2005) 987–996.
[3] L.S. Ashby, K.A. Smith, B. Stea, Gliadel wafer implantation combined with standard radiotherapy and concurrent followed by adjuvant temozolomide for treatment of newly diagnosed high-grade glioma: a systematic literature review, World J. Surg. Oncol. 14 (2016) 225.
[4] R. Stupp, S. Taillibert, A.A. Kanner, S. Kesari, D.M. Steinberg, S.A. Toms, L.P. Taylor, F. Lieberman, A. Silvani, K.L. Fink, Maintenance therapy with tumor-treating fields plus temozolomide vs temozolomide alone for glioblastoma: a randomized clinical trial, JAMA 314 (2015) 2535–2543.
[5] R. Stupp, M.E. Hegi, W.P. Mason, M.J. van den Bent, M.J. Taphoorn, R.C. Janzer, S.K. Ludwin, A. Allgeier, B. Fisher, K. Belanger, Effects of radiotherapy with concomitant and adjuvant temozolomide versus radiotherapy alone on survival in glioblastoma in a randomised phase III study: 5-year analysis of the EORTC-NCIC trial, Lancet Oncol. 10 (2009) 459–466.
[6] E.S. Newlands, G.R.P. Blackledge, J.A. Slack, G.J. Rustin, D.B. Smith, N.S. Stuart, C.P. Quarterman, R. Hoffman, M.F.G. Stevens, M.H. Brampton, A.C. Gibson, Phase I trial of temozolomide (CCRG 81045: M&B 39831: NSC 362856), Br. J. Cancer 65 (1992) 287–291.
[7] A. Azzabi, A.N. Hughes, P.M. Calvert, E.R. Plummer, R. Todd, M.J. Griffin, M.J. Lind, A. Maraveyas, C. Kelly, K. Fishwick, A.H. Calvert, A.V. Boddy, Phase I study of temozolomide plus paclitaxel in patients with advanced malignant melanoma and associated in vitro investigations, Br. J. Cancer 92 (2005) 1006–1012.
[8] L.P. Ganipineni, F. Danhier, V. Preat, Drug delivery challenges and future of chemotherapeutic nanomedicine for glioblastoma treatment, J. Control. Release 281 (2018) 42–57.
[9] C. Bastiancich, J. Bianco, K. Vanvarenberg, B. Ucakar, N. Joudiou, B. Gallez, G. Bastiat, F. Lagarce, V. Préat, F. Danhier, Injectable nanomedicine hydrogel for local chemotherapy of glioblastoma after surgical resection, J. Control. Release 264 (2017) 45–54.
[10] R.W. Chakroun, P. Zhang, R. Lin, P. Schiapparelli, A. Quinones-Hinojosa, H. Cui, Nanotherapeutic systems for local treatment of brain tumors, Wiley Interdiscip. Rev. Nanomed. Nanobiotechnol. 10 (2018) e1479.
[11] F. Mu, J.T. Lucas, J.M. Watts, A.J. Johnson, J.D. Bourland, A.W. Laxton, M.D. Chan, S.B. Tatter, Tumor resection with carmustine wafer placement as salvage therapy after local failure of radiosurgery for brain metastasis, J. Clin. Neurosci. 22 (2015) 561–565.
[12] S.H. Lin, L.R. Kleinberg, Carmustine wafers: localized delivery of chemotherapeutic agents in CNS malignancies, Expert. Rev. Anticancer. Ther. 8 (2008) 343–359.
[13] C. Bastiancich, P. Danhier, V. Préat, F. Danhier, Anticancer drug-loaded hydrogels as drug delivery systems for the local treatment of glioblastoma, J. Control. Release 243 (2016) 29–42.
[14] T. Fourniols, L.D. Randolph, A. Staub, K. Vanvarenberg, J.G. Leprince, V. Préat, A. des Rieux, F. Danhier, Temozolomide-loaded photopolymerizable PEG-DMA-based hydrogel for the treatment of glioblastoma, J. Control. Release 210 (2015) 95–104.
[15] M. Zhao, F. Danhier, C. Bastiancich, N. Joudiou, L.P. Ganipineni, N. Tsakiris, B. Gallez, A. des Rieux, A. Jankovski, J. Bianco, Post-resection treatment of glioblastoma with an injectable nanomedicine-loaded photopolymerizable hydrogel induces long-term survival, Int. J. Pharm. 548 (2018) 522–529.
[16] N. Wauthoz, P. Deleuze, J. Hecq, I. Roland, S. Saussez, I. Adanja, O. Debeir, C. Decaestecker, V. Mathieu, R. Kiss, K. Amighi, In vivo assessment of temozolomide local delivery for lung cancer inhalation therapy, Eur. J. Pharm. Sci. 39 (2010) 402–411.
[17] N.A. Franken, H.M. Rodermond, J. Stap, J. Haveman, C. Van Bree, Clonogenic assay of cells in vitro, Nat. Protoc. 1 (2006) 2315.
[18] Y. Zhao, J.-L. Gao, J.-W. Ji, M. Gao, Q.-S. Yin, Q.-L. Qiu, C. Wang, S.-Z. Chen, J. Xu, R.-S. Liang, Y.-Z. Cai, X.-F. Wang, Cytotoxicity enhancement in MDA-MB-231 cells by the combination treatment of tetrahydropalmatine and berberine derived from Corydalis yanhusuo W. T. Wang, J. Intercult. Ethnopharmacol. 3 (2014) 68–72.
[19] T.-C. Chou, Drug combination studies and their synergy quantification using the Chou-Talalay method, Cancer Res. (2010) 0008–5472. CAN-0009-1947.
[20] P.A. Clark, J.T. Gaal, J.K. Strebe, C.A. Pasch, D.A. Deming, J.S. Kuo, H.I. Robins, The effects of tumor treating fields and temozolomide in MGMT expressing and non-expressing patient-derived glioblastoma cells, J. Clin. Neurosci. 36 (2017) 120–124.
[21] J. Bianco, C. Bastiancich, N. Joudiou, B. Gallez, A. des Rieux, F. Danhier, Novel model of orthotopic U-87 MG glioblastoma resection in athymic nude mice, J. Neurosci. Methods 284 (2017) 96–102.
[22] B. Donnelly, J. Medige, Shear properties of human brain tissue, J. Biomech. Eng. 119 (1997) 423–432.
[23] L. Śliwka, K. Wiktorska, P. Suchocki, M. Milczarek, S. Mielczarek, K. Lubelska, T. Cierpiał, P. Łyżwa, P. Kiełbasiński, A. Jaromin, The comparison of MTT and CVS assays for the assessment of anticancer agent interactions, PLoS One 11 (2016) e0155772.
[24] B. Banelli, A. Daga, A. Forlani, G. Allemanni, D. Marubbi, M.P. Pistillo, A. Profumo, M. Romani, Small molecules targeting histone demethylase genes (KDMs) inhibit growth of temozolomide-resistant glioblastoma cells, Oncotarget 8 (2017) 34896–34910.
[25] M. Hermisson, A. Klumpp, W. Wick, J. Wischhusen, G. Nagel, W. Roos, B. Kaina, M. Weller, O6-methylguanine DNA methyltransferase and p53 status predict temozolomide sensitivity in human malignant glioma cells, J. Neurochem. 96 (2006) 766–776.
[26] C.H. Ryu, W.S. Yoon, K.Y. Park, S.M. Kim, J.Y. Lim, J.S. Woo, C.H. Jeong, Y. Hou, S.-S. Jeun, Valproic acid downregulates the expression of MGMT and sensitizes temozolomide-resistant glioma cells, Biomed. Res. Int. 2012 (2012).
[27] L.D. Mayer, T.O. Harasym, P.G. Tardi, N.L. Harasym, C.R. Shew, S.A. Johnstone, E.C. Ramsay, M.B. Bally, A.S. Janoff, Ratiometric dosing of anticancer drug combinations: controlling drug ratios after systemic administration regulates therapeutic activity in tumor-bearing mice, Mol. Cancer Ther. 5 (2006) 1854–1863.
[28] M. Weller, R. Stupp, G. Reifenberger, A.A. Brandes, M.J. Van Den Bent, W. Wick, M.E. Hegi, MGMT promoter methylation in malignant gliomas: ready for personalized medicine? Nat. Rev. Neurol. 6 (2010) 39.
[29] E.J. Choi, B.J. Cho, D.J. Lee, Y.H. Hwang, S.H. Chun, H.H. Kim, I.A. Kim, Enhanced cytotoxic effect of radiation and temozolomide in malignant glioma cells: targeting PI3K-AKT-mTOR signaling, HSP90 and histone deacetylases, BMC Cancer 14 (2014) 17.
[30] F. Lan, Y. Yang, J. Han, Q. Wu, H. Yu, X. Yue, Sulforaphane reverses chemo-resistance to temozolomide in glioblastoma cells by NF-κB-dependent pathway downregulating MGMT expression, Int. J. Oncol. 48 (2016) 559–568.
[31] Y. Gao, X. Chen, H. Liu, Up-regulation of miR-370-3p restores glioblastoma multiforme sensitivity to temozolomide by influencing MGMT expression, Sci. Rep. 6 (2016) 32972.
[32] D. Zhu, M. Tu, B. Zeng, L. Cai, W. Zheng, Z. Su, Z. Yu, Up-regulation of miR-497 confers resistance to temozolomide in human glioma cells by targeting mTOR/Bcl-2, Cancer Med. 6 (2017) 452–462.
[33] J.W. Hwang, S.M. Noh, B. Kim, H.W. Jung, Gelation and crosslinking characteristics of photopolymerized poly (ethylene glycol) hydrogels, J. Appl. Polym. Sci. 132 (2015).
[34] H. Tan, K.G. Marra, Injectable, biodegradable hydrogels for tissue engineering applications, Materials 3 (2010) 1746–1767.
[35] G.D. Nicodemus, S.J. Bryant, Cell encapsulation in biodegradable hydrogels for tissue engineering applications, Tissue Eng. B Rev. 14 (2008) 149–165.
[36] H.K. Makadia, S.J. Siegel, Poly lactic-co-glycolic acid (PLGA) as biodegradable controlled drug delivery carrier, Polymers 3 (2011) 1377–1397.
[37] A.K. Vellimana, V.R. Recinos, L. Hwang, K.D. Fowers, K.W. Li, Y. Zhang, S. Okonma, C.G. Eberhart, H. Brem, B.M. Tyler, Combination of paclitaxel thermal gel depot with temozolomide and radiotherapy significantly prolongs survival in an experimental rodent glioma model, J. Neuro-Oncol. 111 (2013) 229–236.
[38] S. Ni, X. Fan, J. Wang, H. Qi, X. Li, Biodegradable implants efficiently deliver combination of paclitaxel and temozolomide to glioma C6 cancer cells in vitro, Ann. Biomed. Eng. 42 (2014) 214–221.
[39] Y. Xu, M. Shen, Y. Sun, P. Gao, Y. Duan, Nano composite thermo-sensitive gel for paclitaxel and temozolomide co-delivery to glioblastoma cells, J. Nanosci. Nanotechnol. 16 (2016) 12288–12298.
[40] C. Yoon, N.E. Papadopoulos, L.H. Camacho, S. McIntyre, G.C. Alvarado, A.Y. Bedikian, P. Hwu, K.B. Kim, The clinical efficacy of combination of docetaxel and temozolomide in previously treated patients with stage IV melanoma, Melanoma Res. 20 (2010) 43–47.
[41] A. Azzabi, A. Hughes, P. Calvert, E. Plummer, R. Todd, M. Griffin, M. Lind, A. Maraveyas, C. Kelly, K. Fishwick, Phase I study of temozolomide plus paclitaxel in patients with advanced malignant melanoma and associated in vitro investigations, Br. J. Cancer 92 (2005) 1006.
[42] D. Bafaloukos, H. Gogas, V. Georgoulias, E. Briassoulis, G. Fountzilas, E. Samantas, C. Kalofonos, D. Skarlos, A. Karabelis, P. Kosmidis, Temozolomide in combination with docetaxel in patients with advanced melanoma: a phase II study of the Hellenic Cooperative Oncology Group, J. Clin. Oncol. 20 (2002) 420–425.
[43] Y. Xu, M. Shen, Y. Li, Y. Sun, Y. Teng, Y. Wang, Y. Duan, The synergic antitumor effects of paclitaxel and temozolomide co-loaded in mPEG-PLGA nanoparticles on glioblastoma cells, Oncotarget 7 (2016) 20890–20901.
[44] M. Van Woensel, T. Mathivet, N. Wauthoz, R. Rosière, A.D. Garg, P. Agostinis, V. Mathieu, R. Kiss, F. Lefranc, L. Boon, Sensitization of glioblastoma tumor microenvironment to chemo-and immunotherapy by Galectin-1 intranasal knock-down strategy, Sci. Rep. 7 (2017) 1217.
[45] L. Ding, Q. Wang, M. Shen, Y. Sun, X. Zhang, C. Huang, J. Chen, R. Li, Y. Duan, Thermoresponsive nanocomposite gel for local drug delivery to suppress the growth of glioma by inducing autophagy, Autophagy 13 (2017) 1176–1190.